Simplified Climate Simulation

Felix Hellborg, Rasmus Pernesten
Supervisor: Erik Swietlicki

December 12, 2025

Abstract

With the aim of understanding how a climate model can be constructed and what limitations it will have, we have created a highly simplified climate simulation using programming and mathematical modelling to compute different aspects of a climate system. With a simplified atmosphere and simplified heat transfer, the simulation can in real time show how energy from the Sun is dispersed around the globe.

This model does not aim to predict exact measurements, but rather to reproduce real-world phenomena. Our goal with the model was to observe effects such as day–night cycles, seasonal variations, colder poles and a warmer equator, the Milankovic effect and Hadley circulation. Although the model failed to reproduce all of these features, it is thermally stable, and it clearly shows notable differences between day and night, summer and winter, as well as between equatorial and polar regions. It is also able to capture larger trends, such as the general effect of an increase in greenhouse gases.

Contents

1 Introduction

Climate change is one of the biggest challenges of modern times, posing a threat comparable to that of nuclear war. Enormous resources are therefore allocated to preventing and mitigating the consequences of global warming. To tackle this issue effectively, and to avoid spending time and resources on ineffective measures, climate models are developed.

This paper aims to demonstrate how a simplified climate model can be constructed and what limitations such a model inevitably has. A simplified model cannot predict exact events such as weather patterns or detailed effects of climate change, but many of the underlying ideas are the same as those used in more complex models. Most components of this climate simulation could, in principle, be incorporated into a more accurate climate model if the complexity of the system were increased. For example, heat transfer in this simulation occurs solely through conduction, which is a strong simplification, since atmospheric convection plays a major role in real-world climate dynamics. More limitations of the model will be discussed at the end of the paper, in section 3.2.

Furthermore, the model is designed to test whether simplifying the atmosphere still produces a stable energy level and whether it can recreate real-world phenomena, or if such simplifications would instead lead to runaway effects or unrealistic behaviour such as extreme temperature differences. Since general trends are of greater interest than exact numerical values, several constants and parameters were adjusted to yield realistic behaviour; more on this is explained in Section 3.1. This might appear questionable when discussing whether the mathematical models underlying the simulation function correctly, but we ask the reader to remember that the graphical output serves as an illustration of the model rather than an exact representation of physical reality. For example, the precise magnitude of the temperature increase due to greenhouse gases is less important than the qualitative observation that such an increase occurs, which our model successfully demonstrates.

2 Theory

2.1 Solar System

The solar system model used in the simulation is a simplified model of our own solar system, consisting of only one planet. The parameters of the planet's orbit can be set arbitrarily, including period time T, time at perihelion τ_p, eccentricity e. The planet's motion relative to the star (always located at the origin) adheres to Kepler's laws of planetary motion:

$$x = a(\cos E - e)$$

$$y = b \sin E = a\sqrt{1 - e^2} \sin E$$

where a is the semi-major axis, b is the semi-minor axis, and the eccentric anomaly E is related to the mean anomaly M by

$$M = E - e \sin E$$

where

$$M \equiv n(t - \tau_p).$$

Here, n denotes the average rate of sweep

$$n \equiv \frac{2\pi}{T},$$

and t is the time in arbitrary units since start.

2.2 Mikkola's Approximation

The exact solution to the eccentric anomaly $E(t)$ lacks a general closed form, though, for the purposes of this simulation, the exact solution is irrelevant. There happens to be a very good numerical approximation for $E(t)$ developed by Seppo Mikkola in 1987 [4]. While the details of why this method yields such a highly accurate approximation are beyond the scope of this paper, the full method is presented below.

2.2.1 Formula

Assuming the value of the mean anomaly $M(t)$ is known, Kepler's equation can (in the elliptical case) be rewritten as

$$E(t) = M(t) + e(3s - 4s^3)$$

where

$$s \equiv \sin E(t)/3.$$

The trick lies in approximating s, which can be done by setting

$$\alpha \equiv (1 - e)/(4e + \frac{1}{2})$$

and

$$\beta \equiv \frac{1}{2} M/(4e + \frac{1}{2}).$$

Now let

$$z = (\beta \pm \sqrt{\beta^2 + \alpha^3})^{1/3},$$

choosing the sign of the root term to match the sign of β.

We can, by means of a series expansion approximate s by

$$s \approx z - \frac{\alpha}{z}.$$

Note that M should be chosen as to be in the range $(-\pi, \pi]$ such that it is as close as possible to 0, thus yielding the least error from the series expansion, see [4].

2.3 Heat Equation

The heat equation on a flat cartesian plane can be written as

$$\partial_t T = \kappa \nabla^2 T = \kappa(\partial_{xx}^2 T + \partial_{yy}^2 T)$$

where ∇^2 denotes the Laplacian [7]. In section 2.3.2, we will generalize the heat equation further to be defined on a spherical surface using the Laplace-Beltrami operator. For now, however, we will use the simplest possible geometry to discuss how we can simulate heat diffusion in a discrete system.

2.3.1 Runge-Kutta Methods

Assuming we have discretized the map into a heat matrix T at some time t, we can solve for T at time (t+h) using a system of RK4 calculations [3] [9].

Given an equation

$$\frac{dA}{dt} = F(A, t) \tag{1}$$

where A is a matrix and F is a linear function in the basis of A, and an initial value of $A(t)$, along with a time step h, we can estimate A at the next time step as

$$A(t+h) \approx \frac{h}{6}(k_1 + k_2 + k_3 + k_4) \tag{2}$$

where

$$k_1 = F(A(t)), \tag{3}$$

$$k_2 = F(A(t) + \frac{h}{2}k_1), \tag{4}$$

$$k_3 = F(A(t) + \frac{h}{2}k_2), \tag{5}$$

$$k_4 = F(A(t) + hk_3). \tag{6}$$

The approximation given by RK4 performs significantly better than the familiar Euler method, especially at larger time-steps, allowing us to run the simulation at higher speeds.

Note that for partial differential equations such as the heat equation, we must also discretize (approximate) the second derivatives with respect to coordinates x and y as

$$\partial_{xx}^2 a_{ij} \approx \frac{-a_{i(j+1)} + 2a_{ij} - a_{i(j-1)}}{(\Delta x)^2}$$

and

$$\partial_{yy}^2 a_{ij} \approx \frac{-a_{(i+1)j} + 2a_{ij} - a_{(i-1)j}}{(\Delta y)^2}$$

Here, Δx and Δy refer to the size of the discretization (i.e. the size of each pixel).

2.3.2 Spherical Coordinates

Initially, we wrote the heat equation using the Laplacian ∇^2, which works for geometries lacking any curvature where the metric tensor $g_{\mu\nu}$ is defined on the flat-space $\mathbb{R}^2$ Riemann manifold and the interval is

$$ds^2 = dx^2 + dy^2.$$

In general, we define the metric tensor on a manifold through the interval

$$ds^2 = g_{\mu\nu} dx^\mu dx^\nu.$$

(Note the usage of the Einstein summation convention.)

The heat equation then becomes

$$\partial_t T = \kappa \Delta_g T \tag{7}$$

where Δ_g denotes the Laplace-Beltrami operator which, when applied to some scalar function f, yields [8]

$$\Delta_g f = \frac{1}{\sqrt{|g|}} \partial_i (\sqrt{|g|} g^{ij} \partial_j f). \tag{8}$$

Here, $|g|$ is the absolute value of the determinant of the metric tensor. Again, note the usage of the Einstein summation convention.

In our flat case:

$$g_{\mu\nu} = \begin{pmatrix} 1 & 0 \\ 0 & 1 \end{pmatrix}$$

and $|g|$ is 1. Thus, we can calculate $\Delta_g f$ from equation 8 as

$$\Delta_g f = \partial^2_{x^1 x^1} f + \partial^2_{x^2 x^2} f$$

or in cartesian coordinates

$$\Delta_g f = \partial^2_{xx} f + \partial^2_{yy} f.$$

We're interested in the S^2 Riemann manifold where

$$g_{\mu\nu} = \begin{pmatrix} R^2 & 0 \\ 0 & R^2 \sin^2\theta \end{pmatrix}.$$

Because

$$g_{ij} = 0 \quad \forall \quad i \neq j$$

we find

$$|g| = R^4 \sin^2\theta \Rightarrow \sqrt{|g|} = R^2 \sin\theta \quad \forall \quad \theta \in [0, \pi]$$

and

$$g^{ii} = \frac{1}{g_{ii}}.$$

From equation 8, we find

$$\Delta_{S^2} f = \frac{1}{R^2 \sin\theta}(\partial_\theta(R^2 \sin\theta(g^{\theta\theta}\partial_\theta f)) + (\partial_\phi R^2 \sin\theta(g^{\phi\phi}\partial_\phi f))).$$

Here, we've used the fact that $g^{\theta\phi} = g^{\phi\theta} = 0$ to simplify the expression. We now substitute our values for $g^{\theta\theta}$ and $g^{\phi\phi}$ to find

$$\Delta_{S^2} f = \frac{1}{R^2}(\cot\theta\partial_\theta f + \partial^2_{\theta\theta} f + \frac{1}{\sin^2\theta}\partial^2_{\phi\phi} f).$$

Now, we can rewrite equation 7 as

$$\partial_t T = \kappa\frac{1}{R^2}(\cot\theta\partial_\theta T + \partial^2_{\theta\theta} T + \frac{1}{\sin^2\theta}\partial^2_{\phi\phi} T)$$

which we discretize using

$$\partial_\theta T_{ij} \approx \frac{T_{ij} - T_{i(j-1)}}{\Delta\theta}$$

$$\partial^2_{\theta\theta} T_{ij} \approx \frac{-T_{(i+1)j} + 2T_{ij} - T_{(i-1)j}}{(\Delta\theta)^2}$$

$$\partial^2_{\phi\phi} T_{ij} \approx \frac{-T_{i(j+1)} + 2T_{ij} - T_{i(j-1)}}{(\Delta\phi)^2}$$

2.4 Atmosphere

The atmosphere is arguably the most important and most complex part of any climate model. Without it, calculations and simulations become very simple, and everything can be simplified to black bodies or gray bodies. However, when the object in question is not a stellar body like the Moon, the atmosphere must be taken into account since its composition largely determines the temperature at which equilibrium is reached.

2.4.1 Monte Carlo Method

The Monte Carlo method is the most accurate approach for simulating light traveling through a medium such as the atmosphere. In this method, the path of each photon is simulated individually, and every interaction with the atmosphere is calculated separately. It is therefore highly flexible and can be applied to any medium and at any wavelength, but it is unrealistic for large-scale simulations due to its heavy computational cost. [2]

2.4.2 Flux Transmission Towards the Earth

Since the Monte Carlo method is far too computationally heavy to calculate flux (Power per area unit) within a reasonable time on a planet-sized system, simplifications must be made. We begin by separating the incoming solar radiation

from the outgoing thermal radiation emitted by the planet. In this chapter, we discuss how we model the light approaching the Earth and what happens to it as it passes through the atmosphere.

One important simplification is that we are only interested in the top of the atmosphere, where $\tau_\nu = 0$, and the bottom of the atmosphere, where $\tau_\nu = \tau_\nu^*$, the optical depth of the atmosphere. Everything that happens between these two heights is separated into three cases.

1. The direct flux component is modeled as

$$\pi \mu_0 F_0 e^{-\tau^*/\mu_0} \tag{9}$$

2. The diffuse transmission component, which is scattered multiple times before reaching the surface, is modeled as

$$\pi \mu_0 F_0 t(-\mu_0) \tag{10}$$

3. The diffuse component that is scattered multiple times and reflected between the atmosphere and the surface, which will be addressed soon; see equation 13.

Together, equations 9 and 10 can be combined into

$$T_r(-\mu_0) = t(-\mu) + e^{-\tau^*/\mu_0}. \tag{11}$$

Here, $t(-\mu)$ is approximated by $\frac{\omega \tau^*}{2\mu_0}$, where ω is given by

$$\omega = \frac{\text{diffusion}}{\text{diffusion} + \text{absorption}}.$$

If this expression is multiplied by the incoming flux, we obtain

$$\pi \mu_0 F_0 T_r(-\mu_0) \tag{12}$$

since the solar constant is $F_0 \pi$ and $\mu_0 = \cos(\theta_0)$, where θ_0 is the angle of the incoming radiation measured from the local surface normal. The factor $\pi \mu_0 F_0$ therefore represents the flux at a given point as a function of the solar zenith angle.

This expression applies before any reflections from the surface are taken into account. Because there are theoretically an infinite number of such reflections, they are treated as the convergent series

$$\pi \mu_0 F_0 T_r(-\mu_0) \left[\rho_s \bar{r} + \rho_s^2 \bar{r}^2 + \rho_s^3 \bar{r}^3 + \dots \right] \tag{13}$$

where $\bar{r}$ is the atmospheric albedo without the surface contribution, and ρ_s is the surface albedo. Note that this infinite-reflection model is valid only when the surface is Lambertian, meaning that reflections are assumed to be equally

likely in all directions. Each term in the series represents one additional surface reflection followed by atmospheric scattering: the first term corresponds to a single reflection, the second term to two reflections, and so on. Fortunately, this series is convergent, making it straightforward to evaluate numerically.

$$\begin{aligned} F_T(\mu_0) &= \pi\mu_0 F_0 T_r(-\mu_0)\left[1 + \rho_s\bar{r} + \rho_s^2\bar{r}^2 + \rho_s^3\bar{r}^3 + \dots\right] \\ &= \frac{\pi\mu_0 F_0 T_r(-\mu_0)}{1 - \rho_s\bar{r}} \end{aligned} \tag{14}$$

We now have a fast numerical method to calculate the flux as a function of the angle of incidence $\pi\mu_0 F_0$, the atmospheric albedo $\bar{r}$, and the surface albedo ρ_s [2].

2.5 Heat Radiation

As is well known among those who have studied physics, all bodies radiate energy according to

$$E = \sigma T^4,$$

where E is the emitted energy, σ is the Stefan–Boltzmann constant, and T is the temperature. This is the basic relation used to calculate how much energy is emitted from each point on a surface [5].

However, this expression assumes a perfect blackbody, and since the Earth is certainly not a perfect blackbody, it is more appropriate to treat it as a gray body

$$E = \epsilon\sigma T^4 \tag{15}$$

with $0 < \epsilon < 1$. Another important limitation of this simple radiation model is that it does not account for interactions with the atmosphere, such as scattering, diffusion, and reflection.

3 Simulation

The simulation built during this project is written in Rust using the Bevy game engine [1]. The heat map is represented as a matrix of height 51 and width 161, the idea being that the width is roughly π times greater than the height such that we can project the map using an equirectangular projection onto the spherical planet [6]. The application of physical calculations such as heat absorbtion, black body radiation, and heat diffusion are applied separately, such that their rate can be carefully controlled. Physical constants along with all other parameters of the simulation are stored as constants and can be changed for the purposes of showcasing certain phenomena. The full code for the simulation can be found on Github.

3.1 Units

For the purposes of this project, the units of measurements are not the regular SI-units. Because we're interested in the trends, and the relationships between parameters and outcomes, the values of the simulation parameters have been set such that they yield interesting and realistic results with respect to internal consistency (within the units of measurements we're using, whatever they may be).

When in the course of reading this report, the reader comes across the usage of distance units [D.U.], time units [Ti.U], or temperature units [Te.U.], they should be imagined as corresponding to meters [m], seconds [s], and Kelvin [K] respectively with some arbitrary scaling factor. Note that temperature will always be given in an absolute scale (i.e. starting at zero).

The visual representation should not be thought of as having a realistic scale. The size of a planet with respect to the distance to its host star is so small as to be impossible to see in a realistic relative scale. The same thing is true for the relative difference in size between the planet and the host star itself (the diameter ratio between the earth and the sun is roughly 110:1 [10]).

3.2 Limitations of the Simulation

This simulation uses numerical methods and simplified models to enable it to run in real time. As a consequence, rounding errors occur on top of the inherent limitations of the mathematical models. The model used to calculate light traveling through the atmosphere toward the Earth is fairly accurate as long as the diffuse components do not become too large, which occurs if there are too many clouds [2].

The emission of heat from the planet is simplified by treating the surface as a gray body, which completely ignores the interaction between thermal radiation and the atmosphere. To avoid slowing down the simulation, we also chose not to separate the incoming light into different spectral bands, even though these would interact differently with the atmosphere.

In addition to these mathematical limitations, there are also conceptual ones. Due to its immense complexity, the atmosphere is treated only as a function acting on radiation. In our simulation it has no internal temperature, which removes any heat dissipation through winds or atmospheric circulation.

Due to time limitations, the scope of the simulation had to be restricted. Large climate simulations require computational power at a scale which was simply infeasible for this project, which is why we've scaled down the resolution, distances and update cycles such that it could run on our hardware.

4 Results

After assembling the mathematical models from the theory into a single framework, we simulated the system in several different configurations to examine how various components of the model influence the results.

First, we considered a very simple case: no heat diffusion and a non-rotating planet that orbits its star with an axis perpendicular to the orbital plane. This setup was then made progressively more realistic by adding rotation around the planet's own axis, an elliptical orbit, and a tilted rotational axis.

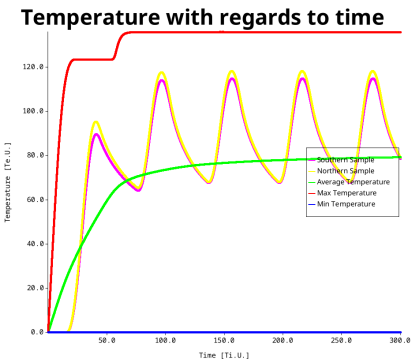

(a) Simulating temperatures on the surface of a non-rotating planet with an axis perpendicular to its orbital plane around its host star, with no heat diffusion. Video link

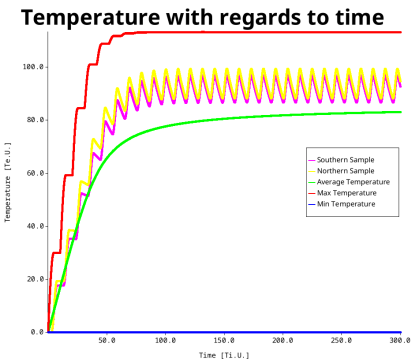

(b) Simulating temperatures on the surface of a rotating planet with an axis perpendicular to its orbital plane around its host star, with no heat diffusion. Video link

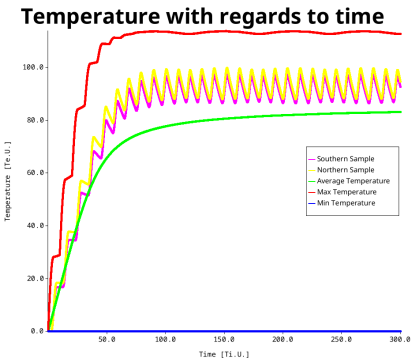

(c) Simulating temperatures on the surface of a rotating planet in an elliptical orbit around its host star, with no heat diffusion. Video link

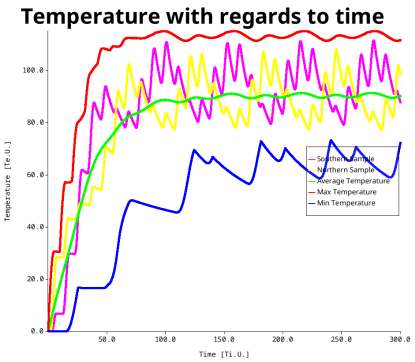

(d) Simulating temperatures on the surface of a rotating planet with a tilted axis and an elliptical orbit, with no heat diffusion. Video link

Figure 1: Overview of the four simulation configurations.

We begin in Figure 1a with a hypothetical planet whose day–night cycle is

determined solely by its revolution around its host star: it experiences half a year of daylight and half a year of darkness. This trend can be seen in the cyclical patterns of the northern and southern samples in the figure. The small temperature differences between the northern and southern samples arise from rounding errors when picking latitudes for the samples and are insignificant.

Since heat diffusion is disabled, the poles remain at their initial temperature (the planet starts with a temperature of zero before reaching equilibrium), which results in the minimum temperature values. The equator, on the other hand, quickly climbs to a stable equilibrium temperature.

In Figure 1b we enable rotation around the planet's own axis, which produces a similar temperature diagram but with much faster day–night cycles.

We then proceed to Figure 1c, where the orbital shape is elliptical, and the day–night cycle remains largely the same, but the maximum temperature now varies periodically. This occurs because the distance between the planet and its host star changes throughout the elliptical orbit (see Section 2.1), and the planet moves through certain parts of the cycle quicker than other parts, meaning that certain parts of the planet will be heated more at certain parts of the orbit.

Finally, in Figure 1d we tilt the planet's rotational axis. We now observe that the northern and southern samples are completely mirrored, which is expected since they still share the same day–night timing but now experience vastly different angles of incidence. We also observe that the minimum temperature changes over time because one of the poles is always slightly tilted toward the star, meaning it no longer has an angle of incidence equal to 90°.

All of this occurs without any diffusion of heat, which produces very sharp and unrealistic results, such as poles that receive no incoming heat. The next step is therefore to enable the heat diffusion methods in the simulation.

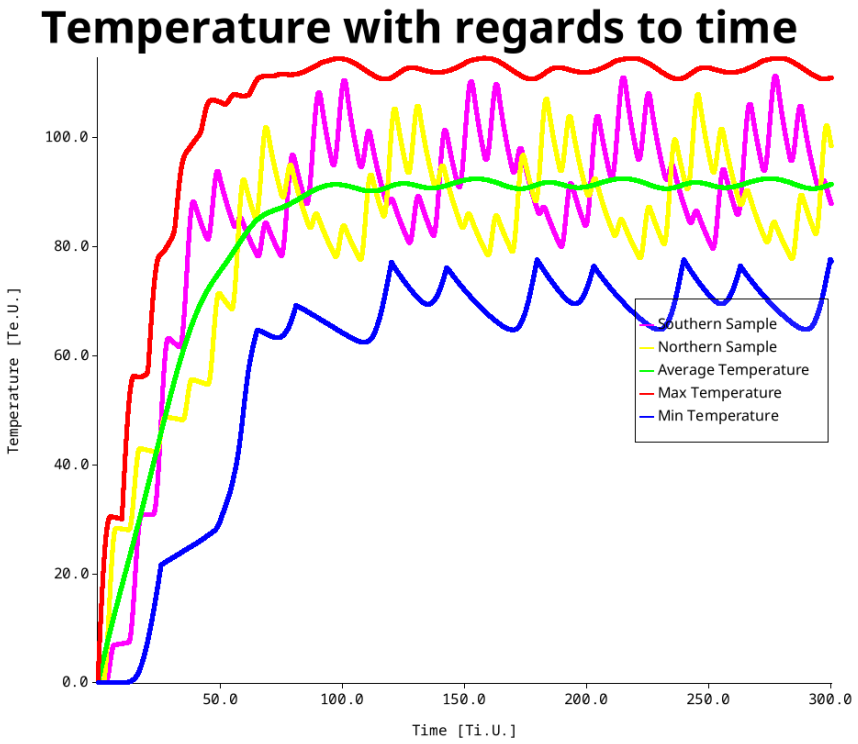

Figure 2: Simulating temperatures on the surface of a rotating planet with a tilted axis and an elliptical orbit, with heat diffusion enabled. Video link

Figure 2 is similar to Figure 1d, but now the minimum temperatures at the poles are more realistic since heat can diffuse across the surface; see Section 2.3.

With this model we can observe many real-world phenomena, and although the simulation is not exact by any means, it can still demonstrate larger-scale trends. For example, we can investigate the effects of drastically increasing greenhouse gas concentrations. In the simulation, this is implemented as a change in the constant determining how much energy can leave the system per unit time.

In Figure 3 we observe a noticeable increase in temperatures across the entire planet, which aligns with real-world expectations.

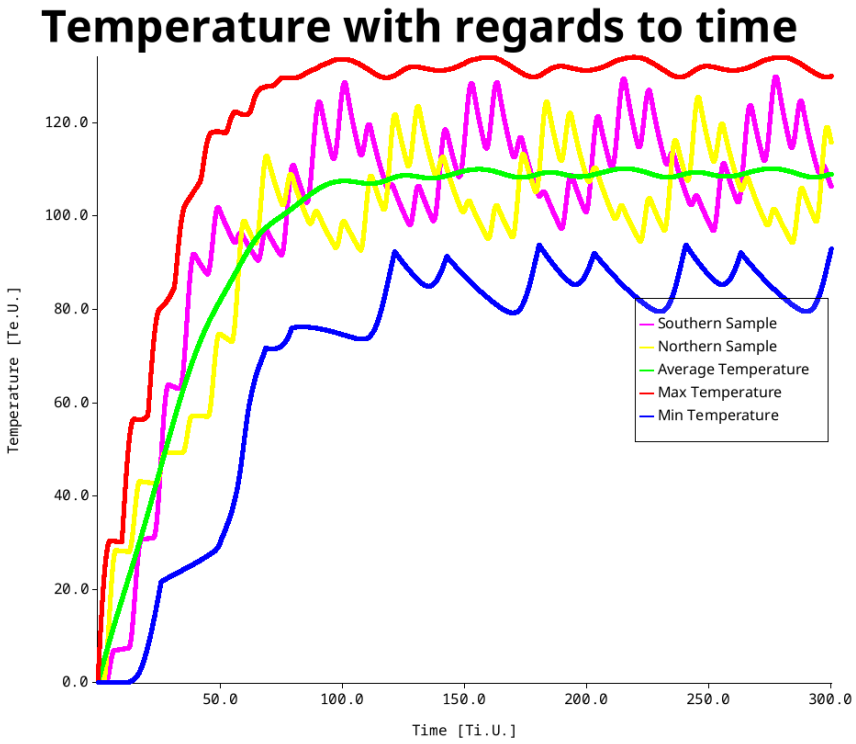

Figure 3: Simulating temperatures on the surface of a rotating planet with a tilted axis and an elliptical orbit, with heat diffusion and an increased amount of greenhouse gases. Video link

5 Conclusion

This project demonstrates how a simplified climate model can capture the fundamental thermodynamic mechanisms governing planetary climate systems. Despite its many simplifications, the simulation reproduces key large-scale phenomena such as day–night cycles, seasonal variations, equator–pole temperature gradients, and the qualitative effect of increased greenhouse gas concentrations.

From a thermodynamic perspective, the results highlight the importance of energy balance in determining long-term climate behavior. Even small changes in the rate at which energy leaves the system can lead to significant shifts in equilibrium temperature, illustrating a core principle behind anthropogenic climate change. While the model does not aim to produce quantitative predictions, it provides conceptual insight into why sustained increases in greenhouse gases pose a long-term risk to climate stability.

Although far from a complete representation of Earth's climate, the model serves as an accessible tool for understanding the physical principles underlying more advanced climate simulations. Such simplified models play an important

role in sustainable development by helping clarify the mechanisms behind climate change and informing the scientific basis for mitigation strategies.

6 Use of AI

Artificial intelligence was used for the following tasks; all results from AI were rigorously checked.

- Spelling checks and grammatical corrections.
- Locating specific pages in long documents when searching for information.
- Finding correct syntax for LaTeX.

References

[1] Bevy Contributors. *Bevy Engine Documentation*. Accessed: 2025-12-11. 2024. URL: https://docs.rs/bevy/0.16.1/bevy/.

[2] James J. Bugla. "Introduction to the Theory of Atmospheric Radiativ Transfer". In: *NASA Reference Publication* (1986), pp. 49–59. URL: https://ntrs.nasa.gov/api/citations/19860018367/downloads/19860018367.pdf.

[3] Wilhelm Kutta. "Beitrag zur näherungsweisen Integration totaler Differentialgleichungen". In: *Zeitschrift für Mathematik und Physik* 46 (1901), pp. 435–453. URL: https://archive.org/details/zeitschriftfrma12runggoog/page/434/mode/2up.

[4] Seppo Mikkola. "A Cubic Approximation For Kepler's Equation". In: *Celestial Mechanics* 40 (1987). ADS bibliographic code: 1987CeMec..40..329M, pp. 329–331. DOI: 10.1007/BF01235850. URL: https://adsabs.harvard.edu/full/1987CeMec..40..329M.

[5] Josef Stefan. "Über die Beziehung zwischen der Wärmestrahlung und der Temperatur". In: *Sitzungsberichte der mathematisch-naturwissenschaftlichen Classe der kaiserlichen Akademie der Wissenschaften* 79.2 (1879), p. 413.

[6] Wikipedia contributors. *Equirectangular projection*. https://en.wikipedia.org/wiki/Equirectangular_projection. Accessed 2025-12-11. 2025.

[7] Wikipedia contributors. *Heat Equation*. https://en.wikipedia.org/wiki/Heat_equation. Accessed: 2025-11-28. 2025.

[8] Wikipedia contributors. *Laplace–Beltrami operator*. https://en.wikipedia.org/wiki/Laplace-Beltrami_operator. Accessed: 2025-12-01. 2025.

[9] Wikipedia contributors. *Runge–Kutta methods*. https://en.wikipedia.org/wiki/Runge-Kutta_methods. Accessed 2025-11-28. 2025.

[10] Wikipedia contributors. *Sun*. https://en.wikipedia.org/wiki/Sun. Accessed: 2025-12-06. 2025.